

Temperature-dependent studies of the geometrically frustrated pyrochlores $\text{Ho}_2\text{Ti}_2\text{O}_7$ and $\text{Dy}_2\text{Ti}_2\text{O}_7$

M. Mączka,¹ M. L. Sanjuán,² A. F. Fuentes,^{2,3} L. Macalik,¹ J. Hanuza,⁴ K. Matsuhira,⁵ and Z. Hiroi⁶

¹*Institute of Low Temperature and Structure Research, Polish Academy of Sciences, P.O. Box 1410, 50-950 Wrocław 2, Poland*

²*Instituto de Ciencia de Materiales de Aragón (Universidad de Zaragoza–CSIC), Facultad de Ciencias, 50009 Zaragoza, Spain*

³*Cinvestav-Salttillo, Apdo. Postal 663, 25000 Saltillo, Coahuila, Mexico*

⁴*Department of Bioorganic Chemistry, University of Economics, 53-345 Wrocław, Poland*

⁵*Faculty of Engineering, Kyushu Institute of Technology, Kitakyushu 804-8550, Japan*

⁶*Institute for Solid State Physics, University of Tokyo, Kashiwa 277-8581, Japan*

(Received 29 January 2009; revised manuscript received 4 May 2009; published 30 June 2009)

A temperature-dependent Raman study of $\text{Ho}_2\text{Ti}_2\text{O}_7$ and $\text{Dy}_2\text{Ti}_2\text{O}_7$ single crystals was performed in the 5–873 K temperature range. Polarized spectra allowed us to establish the symmetries of the observed bands and revise the mode assignment made in previous works. Our studies revealed also two additional bands near 287 and 300 cm^{-1} for $\text{Dy}_2\text{Ti}_2\text{O}_7$, which can be assigned to crystal field transitions in Dy^{3+} ions. Temperature dependent Raman studies showed large increase of linewidths. These changes have been analyzed in terms of strong third-order phonon-phonon anharmonic interactions. The Raman spectra also showed anomalous softening of the majority of phonon modes upon cooling in the whole temperature range studied. In contrast to this behavior, the F_{2g} $\sim 310 \text{ cm}^{-1}$ and E_g $\sim 330 \text{ cm}^{-1}$ phonon modes showed hardening upon cooling down to about (100–120 K) and then anomalous softening below this temperature. This anomalous behavior of phonon wave numbers has been attributed to the increase in octahedral distortion upon cooling.

DOI: [10.1103/PhysRevB.79.214437](https://doi.org/10.1103/PhysRevB.79.214437)

PACS number(s): 75.50.Lk, 63.20.dd, 71.70.Ch

I. INTRODUCTION

Rare-earth metal titanates, with formula $\text{A}_2\text{Ti}_2\text{O}_7$, belong to a family of geometrically frustrated magnetic insulators, crystallizing in the pyrochlore structure.¹ While the exchange between the rare-earth spins is antiferromagnetic for almost all the titanate pyrochlores,² the difference in the on site anisotropy and presence of dipolar interactions or spin fluctuations leads to significant differences in the magnetic properties of these materials. For instance, $\text{Dy}_2\text{Ti}_2\text{O}_7$ and $\text{Ho}_2\text{Ti}_2\text{O}_7$ have weak ferromagnetic coupling, which may be largely dipolar in origin, and they show spin ice behavior.^{3–6} $\text{Gd}_2\text{Ti}_2\text{O}_7$ and $\text{Er}_2\text{Ti}_2\text{O}_7$ have predominantly antiferromagnetic coupling and they exhibit antiferromagnetic ordering at very low temperatures.^{7–9} In contrast to other rare-earth titanates, $\text{Tb}_2\text{Ti}_2\text{O}_7$ does not order magnetically, and remains the only true cooperative paramagnet down to at least 70–20 mK, despite an antiferromagnetic Curie-Weiss temperature $\sim -18 \text{ K}$.^{10–12}

$\text{Ho}_2\text{Ti}_2\text{O}_7$ and $\text{Dy}_2\text{Ti}_2\text{O}_7$ have been the subject of many studies.^{3,5,13–18} Extended x-ray absorption fine structure (EXAFS) and x-ray diffraction studies showed that $\text{Ho}_2\text{Ti}_2\text{O}_7$ is well ordered and the cubic structure remains stable down to liquid helium temperature.^{13,14} Recent powder x-ray diffraction studies of $\text{Dy}_2\text{Ti}_2\text{O}_7$ suggested this material undergoes a subtle structural transformation, with no change of space group, near 110 K.¹⁸ Muon-spin rotation data indicated lack of magnetic ordering in $\text{Ho}_2\text{Ti}_2\text{O}_7$ down to about 50 mK and neutron scattering as well as heat capacity results indicated unambiguously that $\text{Ho}_2\text{Ti}_2\text{O}_7$ and $\text{Dy}_2\text{Ti}_2\text{O}_7$ exhibit spin ice correlations at low temperature.^{3,5,15} It was also shown that the short-range magnetic correlation becomes significant in $\text{Ho}_2\text{Ti}_2\text{O}_7$ with decreasing temperature at around 30 K.¹⁶

Raman spectroscopy has been widely used in studies of pyrochlore-type materials since this method may provide very useful information on disorder, spin-phonon and crystal field (CF)–phonon interactions.^{17–25} In a previous paper we reported the results of temperature-dependent Raman scattering studies of $\text{Gd}_2\text{Ti}_2\text{O}_7$ and $\text{Er}_2\text{Ti}_2\text{O}_7$, which order magnetically at very low temperature.²⁶ These studies revealed anomalous softening of some modes below 130–100 K.²⁶ Very recently, we reported detailed temperature dependence of Raman modes for the spin liquid pyrochlore $\text{Tb}_2\text{Ti}_2\text{O}_7$, which revealed presence of unusually strong CF-phonon interactions.²⁷ The present paper reports temperature-dependent Raman studies of $\text{Ho}_2\text{Ti}_2\text{O}_7$ and $\text{Dy}_2\text{Ti}_2\text{O}_7$, which belong to the third subgroup of rare-earth titanates exhibiting spin ice behavior. Nonpolarized Raman scattering studies of $\text{Dy}_2\text{Ti}_2\text{O}_7$ in the 12–300 K range were reported recently.¹⁸ However, we will show that our present results give significant information due to the fact that we have studied polarized spectra in a much broader temperature range (5–873 K). We present also new polarized spectra for $\text{Gd}_2\text{Ti}_2\text{O}_7$ single crystal as well as optical absorption and luminescence spectra of $\text{Dy}_2\text{Ti}_2\text{O}_7$. The aim of these studies was to obtain information on symmetries of modes, their nature (i.e., whether they correspond to fundamentals, overtones or CF transitions), temperature dependence and energies of Stark levels of the ground manifold. These results will be compared to the literature data available for other rare-earth titanates in order to see if the significant change in magnetic properties is reflected in the phonon properties of these materials.

The peculiarities of the pyrochlore lattice, in particular the relevance of the oxygen free parameter, x , are also discussed in connection with the thermal evolution of the linewidths and shifts of the Raman bands.

II. EXPERIMENTAL

Single crystals of $\text{Ho}_2\text{Ti}_2\text{O}_7$ and $\text{Dy}_2\text{Ti}_2\text{O}_7$ were prepared by the floating-zone method using an infrared furnace equipped with four halogen lamps and elliptical mirrors. The crystals were grown under O_2 gas flow to avoid oxygen deficiency (typical growth rate 4 mm/h).

Raman spectra were measured in the 5–873 K range using a Dilor XY spectrometer with a charge coupled device (CCD) detector and the 514.5 nm excitation line of an argon laser. The spectral resolution was 2 cm^{-1} . Backscattering configuration was used in all measurements.

The optical absorption spectra of polished samples were measured at 300 and 8 K using a Cary 5E Varian spectrophotometer equipped with a continuous flow helium cryostat. The spectral resolution was 0.1 nm in the visible and 0.8 nm in the near-infrared (near-IR) region.

Near-IR luminescence was recorded with a FT-Raman spectrometer Bruker RFS 100. A diode-pumped Nd:YAG laser, emitting at 1064 nm, was used as an excitation source. The signal was detected with a Germanium detector and the spectral resolution was 2 cm^{-1} .

III. RESULTS AND DISCUSSION

A. Selection rules and assignment of phonon modes

According to a group theoretical analysis, a pyrochlore $\text{A}_2\text{B}_2\text{O}(1)_6\text{O}(2)$ compound (space group 227, $Fd\bar{3}m$) should have six Raman-active fundamental modes distributed among $\text{A}_{1g} + \text{E}_g + 4\text{F}_{2g}$ irreducible representations.²⁸ Since A and B cations occupy sites with inversion symmetry, only O(1) and O(2) atoms participate in Raman-active modes.

The polarized Raman spectra of $\text{Ho}_2\text{Ti}_2\text{O}_7$ and $\text{Dy}_2\text{Ti}_2\text{O}_7$ at a few temperatures are presented in Figs. 1 and 2, respectively, and the observed wave numbers are listed in Table I. The polarized room temperature spectra of $\text{Gd}_2\text{Ti}_2\text{O}_7$ are also presented in Fig. 2 for the comparison sake. These spectra were corrected by the Bose-Einstein occupation factor for Stokes processes $[n(\omega) + 1]$, where $n(\omega) = 1/[\exp(\hbar\omega/k_B T) - 1]$. The spectra of $\text{Ho}_2\text{Ti}_2\text{O}_7$ in the 5–300 K range were measured in back-scattering geometry for the crystal with face perpendicular to $[1-10]$. This direction will henceforth be denoted x' . The incident light was polarized parallel to $[111]$, which will be denoted y' . Polarization of the scattered light was either parallel to y' or parallel to $[-1-12]$, which will be denoted z' . The spectra of $\text{Ho}_2\text{Ti}_2\text{O}_7$ above 300 K were measured on the same plane but with the incident light polarized parallel to $[001]$ (z direction) and scattered light polarized either parallel to z or parallel to $[110]$, which will be denoted y'' . This is also the configuration used for RT measurements of $\text{Gd}_2\text{Ti}_2\text{O}_7$. Raman spectra of $\text{Dy}_2\text{Ti}_2\text{O}_7$ were measured in back-scattering geometry onto the face perpendicular to $[100]$ (x direction). The incident light was polarized parallel to $[001]$ (z direction) and the scattered light was polarized either parallel to z or parallel to $[010]$ (y direction).

The relative intensities of the modes can be calculated from the Raman polarizability tensors appropriate for the O_h symmetry of pyrochlores.²⁹ Table II lists the intensities of the

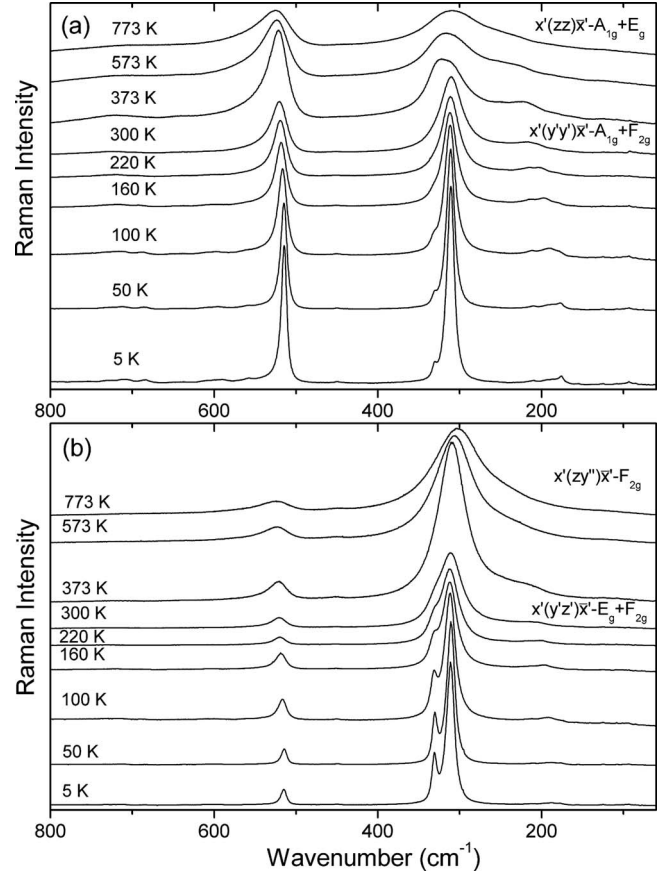


FIG. 1. Polarized Raman spectra of $\text{Ho}_2\text{Ti}_2\text{O}_7$ single crystal at a few temperatures.

Raman modes in each of the applied configurations. In the $x(z y) x$ and $x'(z y'') x'$ configurations only F_{2g} modes and in the $x(z z) x$ and $x'(z z) x'$ configurations both the A_{1g} and E_g modes should appear. In order to discriminate between the A_{1g} and E_g modes, the $x'(y' y') x'$ and $x'(y' z') x'$ configurations can be used because in the former configuration the E_g and in the latter the A_{1g} mode should disappear.

According to literature data for rare-earth titanates, the bands near 310 , 330 and 520 cm^{-1} can be assigned to the F_{2g} , E_g , and A_{1g} modes, respectively.^{2,17–19,26–28,30–32} The polarization behavior presented in Figs. 1 and 2 confirms this assignment. However, the observed modes do not disappear completely in the forbidden configurations possibly due to the use of a microscope or slight misalignment of the samples. It is worth adding that according to Lummen *et al.*¹⁷ no Raman spectrum of any of the rare-earth titanates fulfilling their selection rules has been published. Our present results show, however, that the selection rules are well fulfilled, especially for $\text{Dy}_2\text{Ti}_2\text{O}_7$ and $\text{Gd}_2\text{Ti}_2\text{O}_7$.

The location of the remaining three F_{2g} modes is not straightforward since the literature data are not consistent due to at least two reasons. First, the F_{2g} modes are weak and Raman spectra of pyrochlores show presence of many weak bands corresponding not only to fundamental transitions but also to second-order scattering and CF transitions. Second, nearly all available data were obtained for polycrystalline samples and therefore symmetries of the observed modes

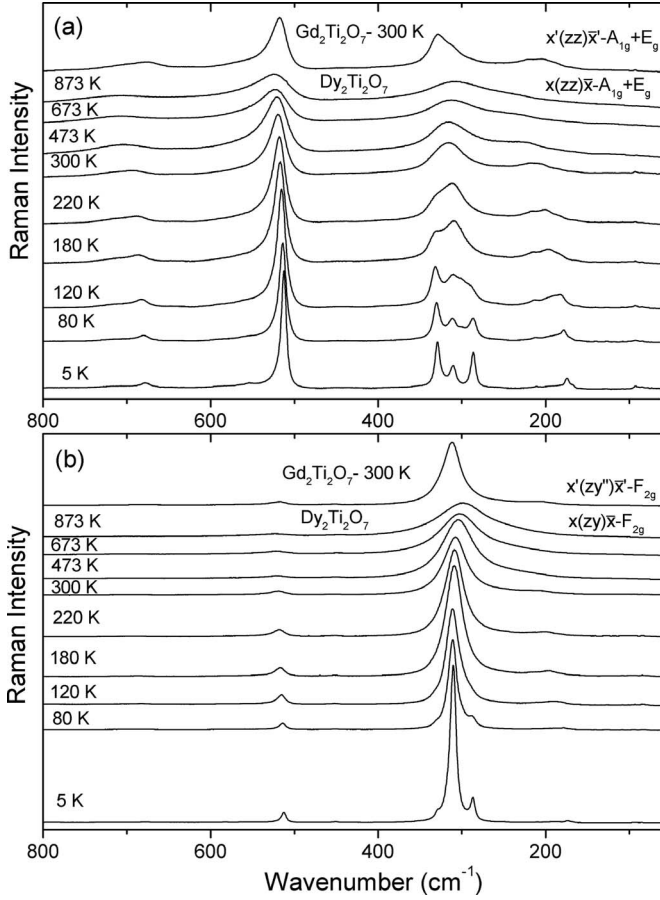


FIG. 2. Polarized Raman spectra of $\text{Dy}_2\text{Ti}_2\text{O}_7$ single crystal at a few temperatures and room temperature spectra of $\text{Gd}_2\text{Ti}_2\text{O}_7$.

TABLE I. A list of experimental wave numbers in cm^{-1} at 5 and 300 K together with proposed assignment. For the comparison sake, recent literature values and assignment for $\text{Dy}_2\text{Ti}_2\text{O}_7$ at 12 K (Ref. 18) are also presented. * Value at 120 K.

$\text{Ho}_2\text{Ti}_2\text{O}_7$			$\text{Dy}_2\text{Ti}_2\text{O}_7$			Assignment	$\text{Dy}_2\text{Ti}_2\text{O}_7$	
5 K	300 K	sym.	5 K	300 K	sym.		(Ref. 18)	Assignment (Ref. 18)
176	183	A_{1g}	175	186	A_{1g}	Overtone	174	Phonon F_{2g}
189	203	$A_{1g}+F_{2g}$	190	205	$A_{1g}+F_{2g}$	Overtone+	194	Phonon (IR)
						Phonon F_{2g}		
210	216	A_{1g}	211	217	A_{1g}	Overtone		
			287			CF	287	Phonon
			300*			CF		
311	310	F_{2g}	311	307	F_{2g}	Phonon F_{2g}	312	Phonon F_{2g}
331	331	E_g	329	327	E_g	Phonon E_g	330	Phonon E_g
450	451	F_{2g}	450	452	F_{2g}	Phonon F_{2g}	453	Phonon F_{2g}
514	520	A_{1g}	513	519	A_{1g}	Phonon A_{1g}	515	Phonon A_{1g}
558		A_{1g}	554		A_{1g}	Overtone	563	Phonon F_{2g}
			583	581	F_{2g}	Phonon F_{2g}		
591		A_{1g}	585	588	A_{1g}	Overtone		
684		A_{1g}	678	690	A_{1g}	Overtone	680	Phonon (second-order)
709	722	A_{1g}	707	710	A_{1g}	Overtone	712	Phonon (second-order)
728		A_{1g}				Overtone		

TABLE II. Intensity of the Raman-active modes in different backscattering configurations for the O_h symmetry.

Compound	Configuration	A_{1g}	E_g	F_{2g}
$\text{Ho}_2\text{Ti}_2\text{O}_7$	$x'(y'y')x'$	a^2	0	$4/3c^2$
	$x'(y'z')x'$	0	$2b^2$	$1/3c^2$
$\text{Ho}_2\text{Ti}_2\text{O}_7$ and $\text{Gd}_2\text{Ti}_2\text{O}_7$	$x'(zz)x'$	a^2	$4b^2$	0
	$x'(zy'')x'$	0	0	c^2
$\text{Dy}_2\text{Ti}_2\text{O}_7$	$x(zz)x$	a^2	$4b^2$	0
	$x(zy)x$	0	0	c^2

could not be established. Moreover, a few single crystal Raman studies also did not show clear polarization behavior of Raman bands, as emphasized by Lummen *et al.*¹⁷ Thus the three weak F_{2g} modes at room temperature were located at 203, 509, and 540 cm^{-1} for $\text{Sm}_2\text{Ti}_2\text{O}_7$,² near 205–214, 256–297, and 550–562 cm^{-1} for $\text{A}_2\text{Ti}_2\text{O}_7$ ($A=\text{Gd}, \text{Tb}, \text{Dy}, \text{Ho}$),¹⁷ 220–225, 517–531, and 580–590 cm^{-1} for $\text{A}_2\text{Ti}_2\text{O}_7$ ($A=\text{Y}, \text{Sm}, \text{Gd}, \text{Yb}$),³⁰ and at 219, 455, and 549 cm^{-1} for $\text{Gd}_2\text{Ti}_2\text{O}_7$.¹⁹ Recently, these three modes were located at 174, 453, and 563 cm^{-1} for $\text{Dy}_2\text{Ti}_2\text{O}_7$ at 12 K.¹⁸ In our previous Raman studies of polycrystalline $\text{A}_2\text{Ti}_2\text{O}_7$ pyrochlores ($A=\text{Gd}, \text{Er}, \text{Dy}, \text{Tb}$) we assigned the room temperature bands near 205–240 and 558–565 cm^{-1} to the F_{2g} modes and we concluded that the third F_{2g} mode can be located either near 450 or 580 cm^{-1} .^{26,27} In the present work, in order to better observe polarization of the bands, the $x(zy)x$ and $x'(y'z')x'$ spectra corresponding to the F_{2g} and $F_{2g}+E_g$ modes, respectively, were corrected by subtracting from the measured spectra the part corresponding to the polarization leakage. We have assumed that all intensity of the band near

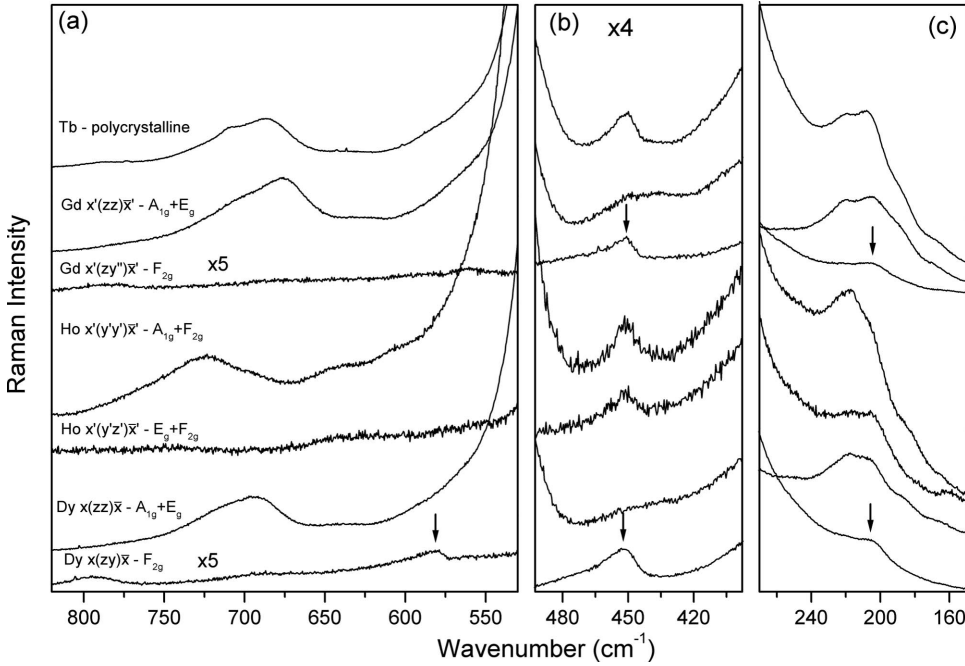


FIG. 3. Enlarged parts of the polarized room temperature Raman spectra of $\text{Dy}_2\text{Ti}_2\text{O}_7$, $\text{Ho}_2\text{Ti}_2\text{O}_7$, and $\text{Gd}_2\text{Ti}_2\text{O}_7$ showing presence of weak bands. For the comparison sake, the Raman spectrum of the polycrystalline $\text{Tb}_2\text{Ti}_2\text{O}_7$ sample is also presented. All spectra in panel (b) were multiplied by 4. The $x(z'y)x$ spectrum of $\text{Dy}_2\text{Ti}_2\text{O}_7$ and the $x'(zy'')x'$ spectrum of $\text{Gd}_2\text{Ti}_2\text{O}_7$ in panel (a) were multiplied by 5. Arrows indicate positions of weak F_{2g} modes.

520 cm^{-1} is a leakage. The resulting spectra are presented in Figs. 3 and 4 for room and low temperature, respectively. They clearly show that at room temperature only the bands at about 205 (206), 452 (451) and 581 cm^{-1} for $\text{Dy}_2\text{Ti}_2\text{O}_7$ ($\text{Gd}_2\text{Ti}_2\text{O}_7$) have F_{2g} symmetry and they should be assigned to the three expected fundamental modes. These bands are observed at 190, 450 and 583 cm^{-1} for $\text{Dy}_2\text{Ti}_2\text{O}_7$ at 5 K (see Fig. 4 and Table I). Our results show therefore that the assignment of the 450 cm^{-1} band is in agreement with the recent studies of Saha *et al.*¹⁸ but Saha's assignment of the bands near 554 and 175 cm^{-1} (at 5 K) to the F_{2g} modes is incorrect. It is worth noting that in the Raman spectra of polycrystalline samples the 450 cm^{-1} band can be obscured by very

similar band of TiO_2 (rutile) impurity.³³ However, this impurity should also give rise to a Raman band near 608 cm^{-1} ,³³ which is absent in the Raman spectra of single crystals. The assignment of the band at about 450 cm^{-1} is also supported by the calculations of Hess *et al.*¹⁹ who predicted a band near 467 cm^{-1} for $\text{Gd}_2\text{Ti}_2\text{O}_7$, and Raman studies of $\text{Y}_2\text{Ru}_2\text{O}_7$ and $\text{Y}_2\text{Mn}_2\text{O}_7$ pyrochlores, which exhibited the strongest A_{1g} and F_{2g} modes at similar wave numbers as the rare-earth titanates and a very clear F_{2g} mode near $410\text{--}456\text{ cm}^{-1}$.^{34,35}

Our polarized spectra show also the presence of a number of extra bands at 205, 210, and $650\text{--}750\text{ cm}^{-1}$ which have A_{1g} symmetry at room temperature (see Table I). Extra A_{1g} bands are also found at low temperature, as seen in Figure 4.

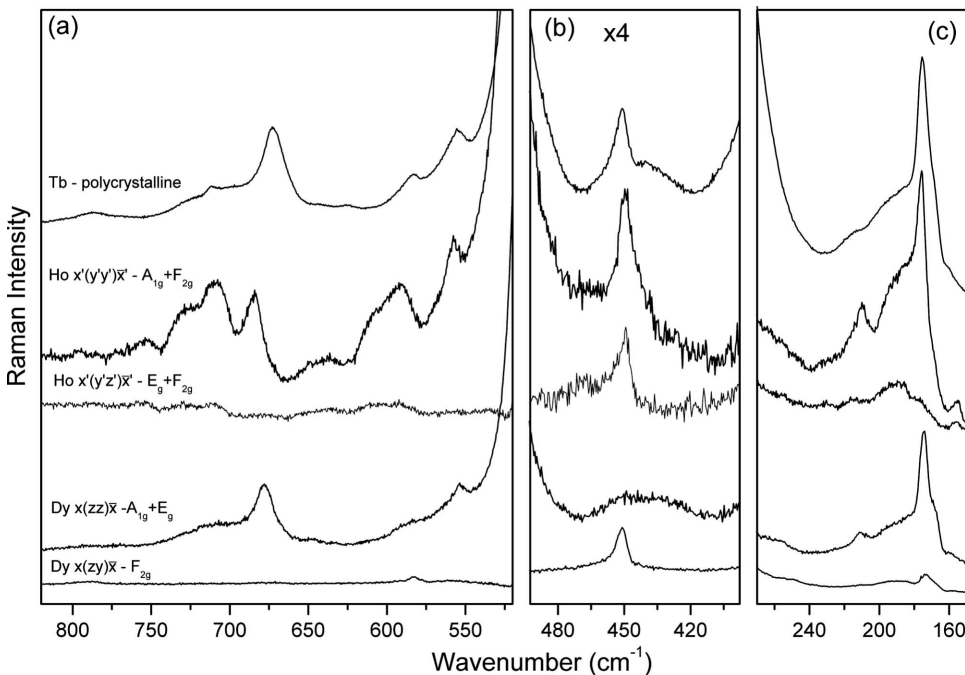


FIG. 4. Enlarged parts of the polarized Raman spectra of $\text{Dy}_2\text{Ti}_2\text{O}_7$ and $\text{Ho}_2\text{Ti}_2\text{O}_7$ at 5 K showing presence of weak bands. For the comparison sake, the Raman spectrum of the polycrystalline $\text{Tb}_2\text{Ti}_2\text{O}_7$ sample at 45 K is also presented. All spectra in panel (b) were multiplied by 4.

These bands cannot be assigned to CF transitions since they are observed also for $\text{Gd}_2\text{Ti}_2\text{O}_7$ although there is no a level splitting due to the local CF for this material. They can neither be assigned to any fundamental, since the unique A_{1g} mode expected is detected at 520 cm^{-1} . They are, therefore, attributed to second-order excitations. Moreover, their A_{1g} symmetry suggests that they arise mainly from phonon overtones. Unfortunately, phonon density of states is not known for the rare-earth titanates and therefore we cannot propose more detailed assignment of the observed overtones. We can only suggest that the overtones below 220 cm^{-1} range are most likely due to Brillouin zone boundary acoustic modes. Since the modes at $670\text{--}730\text{ cm}^{-1}$ have purely A_{1g} character, they are most likely overtones of the A_{2u} modes. This conclusion is consistent with our lattice dynamics calculations (not discussed in this paper) which predicted that one of the A_{2u} modes should be observed near $330\text{--}340\text{ cm}^{-1}$. It is worth noting that Saha *et al.*¹⁸ assigned a band near 194 cm^{-1} (at 12 K) to an infrared active or silent mode rendered Raman active due to lowering of the local symmetry. This band corresponds mainly to our broad A_{1g} band at 190 cm^{-1} . Our polarized spectra show that all A_{1g} modes near 200 cm^{-1} can be assigned to overtones.

It is worth noting that the A_{1g} band near 520 cm^{-1} is clearly asymmetric (see Figs. 1 and 2). This asymmetry is also very clearly seen in the spectra presented in the literature, although nobody mentioned about this characteristic feature. The attribution of most of the spectrum above 550 cm^{-1} to the second-order phonon scattering provides a straightforward explanation for the asymmetry of the A_{1g} band as due to the third-order coupling between the A_{1g} mode at about 520 cm^{-1} and the two-phonon density of states. It has been suggested in other ordered-vacancy compounds that the presence of such vacancies yields a highly anharmonic vibrational potential and enhances the phonon-phonon coupling.³⁶ This explanation also holds for the pyrochlores, where one-eighth of the oxygen positions remain empty at site 8a (origin at B atom). Since the second-order phononic continuum has mostly A_{1g} character, no asymmetry appears for the E_g or F_{2g} modes in the $300\text{--}330\text{ cm}^{-1}$ range.

B. Origin of the 287 cm^{-1} mode of $\text{Dy}_2\text{Ti}_2\text{O}_7$

The comparison of the Raman spectra recorded for $\text{Dy}_2\text{Ti}_2\text{O}_7$ with the spectra of $\text{Ho}_2\text{Ti}_2\text{O}_7$ and previously studied $\text{Gd}_2\text{Ti}_2\text{O}_7$ and $\text{Er}_2\text{Ti}_2\text{O}_7$ shows that at low temperatures an additional band appears at 287 cm^{-1} , which is not observed for the other rare-earth titanates (see Fig. 5). Lummen *et al.*¹⁷ tentatively assigned this band to CF transition. However, it was proposed recently that this band should be assigned to a new phonon mode appearing due to lowering of the site symmetries arising from local structural deformation below 110 K.¹⁸ It also was argued that this band should be assigned to a phonon mode since it showed 4 cm^{-1} shift when ^{16}O is replaced by ^{18}O and the bandwidth is less in ^{18}O rich $\text{Dy}_2\text{Ti}_2\text{O}_7$ as compared to its value in ^{16}O rich $\text{Dy}_2\text{Ti}_2\text{O}_7$.¹⁸

As can be seen in Fig. 2, the 287 cm^{-1} band is not well polarized, i.e., it is slightly more intense in the $x(zz)x$ con-

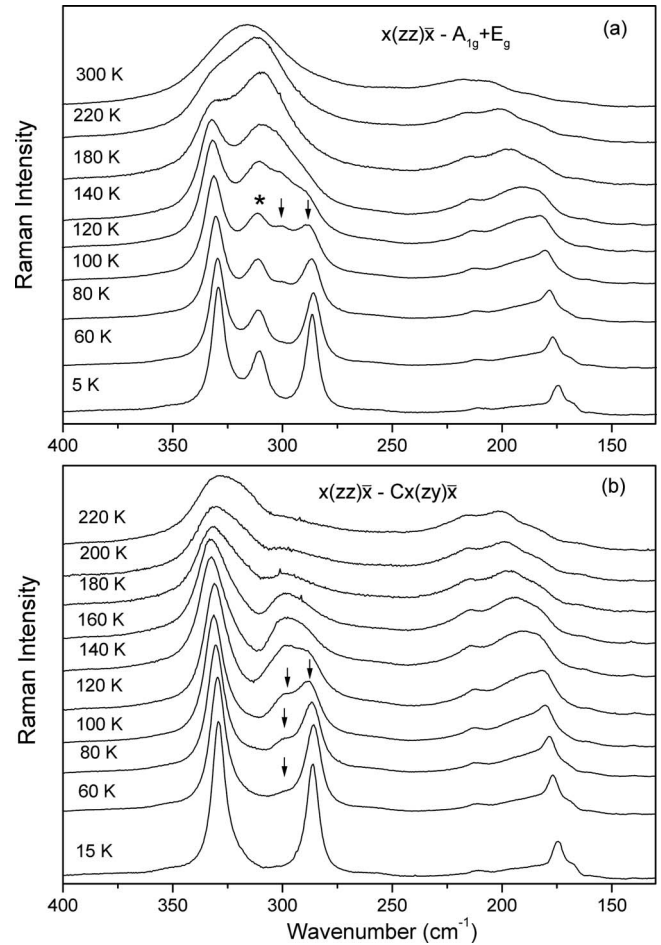


FIG. 5. (a) Enlarged part of the $x(zz)x$ Raman spectra of $\text{Dy}_2\text{Ti}_2\text{O}_7$ showing temperature dependence of the low wave number bands. Panel (b) shows the difference spectra after subtracting the part due to polarization leakage (C is a small coefficient near 0.1). Bands which can be assigned to CF transitions are indicated by arrows and the asterisk indicates the band appearing due to leakage.

figuration ($A_{1g}+E_g$ symmetry) than in the $x(zy)x$ configuration (F_{2g} symmetry). The ratio of intensity for these configurations is 1.3 at 5 K. This result shows clearly that the intensity pattern of this band is quite different from that of the phonon modes of symmetry A_{1g} , F_{2g} , and E_g . One can also notice that intensity of this band decreases and its linewidth increases significantly upon heating but it does not disappear at 110 K, as suggested by Saha *et al.*¹⁸ (this band is still observed at 160 K as a shoulder at about 293 cm^{-1} , see Fig. 5). This polarization behavior and the temperature dependence suggest that the 287 cm^{-1} band is not related to any one- or two-phonon scattering. We have, therefore, decided to check if this feature could be explained as resulting from a CF excitation. The data on CF levels in $\text{Dy}_2\text{Ti}_2\text{O}_7$ are not conclusive since calculations of Jana *et al.*³⁷ predicted that there are no CF levels in the $190\text{--}442\text{ cm}^{-1}$ range whereas Rosenkratz *et al.*³⁸ estimated the first excited state at approximately 266 cm^{-1} . Recent heat capacity studies of Saha *et al.*¹⁸ suggested that the position of first excited CF split doublet is close to 240 cm^{-1} . To check if there are any

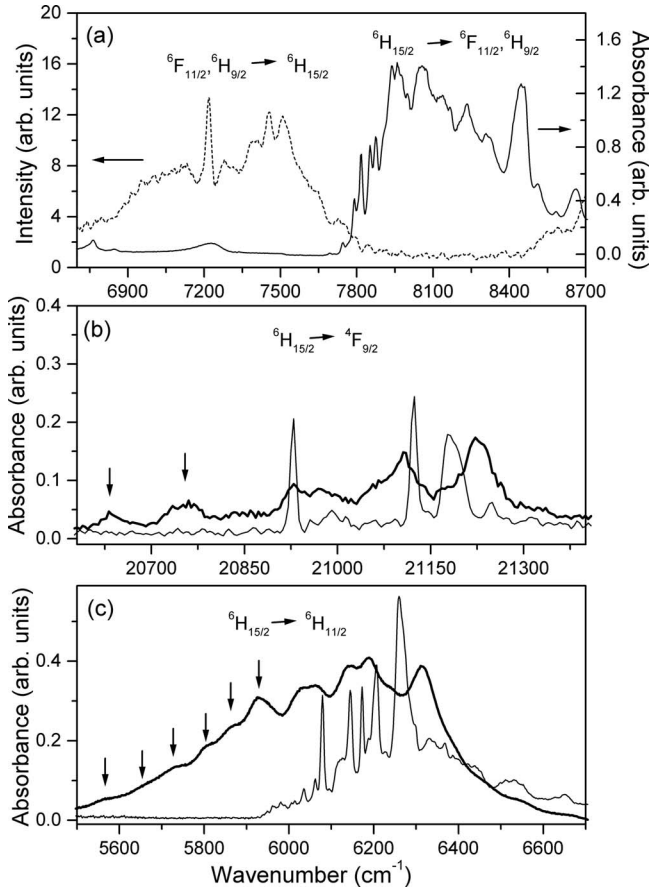


FIG. 6. (a) The absorption (8 K) and luminescence (5 K) spectra of $\text{Dy}_2\text{Ti}_2\text{O}_7$ corresponding to transitions between the ground manifold ${}^6\text{H}_{15/2}$ and the excited manifolds ${}^6\text{F}_{11/2} + {}^6\text{H}_{9/2}$. Panels (b) and (c) show the absorption spectra at 300 (thick lines) and 5 K (thin lines) corresponding to transitions from the ground manifold ${}^6\text{H}_{15/2}$ to the excited manifolds ${}^4\text{F}_{9/2}$ and ${}^6\text{H}_{11/2}$, respectively. Arrows indicate positions of “hot” bands.

CF levels near 280–300 cm^{-1} , we have measured absorption spectra of $\text{Dy}_2\text{Ti}_2\text{O}_7$ at 8 and 300 K and the luminescence spectrum at 4.2 K. The part corresponding to transitions between the ground manifold ${}^6\text{H}_{15/2}$ and the excited manifolds ${}^6\text{F}_{11/2} + {}^6\text{H}_{9/2}$ is presented in Fig. 6(a). Although the luminescence is weak due to concentration quenching, clear bands can be observed at 7507, 7455, 7391, 7280, and 7218 cm^{-1} . We assign the absorption line at 7746 cm^{-1} to the transition between the ground levels of the ${}^6\text{H}_{15/2}$ and ${}^6\text{H}_{9/2}$ manifolds (0-0 transition) and thus six Stark levels of the ground manifold ${}^6\text{H}_{15/2}$ are at 0, 239, 291, 355, 466, and 528 cm^{-1} . Since the ground manifold ${}^6\text{H}_{15/2}$ should split into eight Stark levels (see discussion below), two levels were not observed in the luminescence spectrum. We have therefore attempted to estimate energies of these missing Stark levels from energies of “hot” bands. Figures 6(b) and 6(c) show the absorption spectra corresponding to transitions into the excited manifolds ${}^4\text{F}_{9/2}$ and ${}^6\text{H}_{11/2}$. In the first case the 0-0 transition is observed at 20929 cm^{-1} and the hot bands at 20751 and 20635 cm^{-1} . The difference between the energy of the 0-0 transition and the two hot bands yields 178 and 294 cm^{-1} . In the second case the hot bands are observed at 5941, 5857,

5807, 5735, 5669, and 5565 cm^{-1} and the 0-0 transition at 6065 cm^{-1} yielding the energy difference of 94, 178, 228, 300, 366, and 470 cm^{-1} . We have used in this estimation the energies of hot bands found at 300 K and the 0-0 bands observed at 5 K because the former bands are not observed at 5 K and the latter at 300 K. Since energy of CF transitions is expected to increase by a few cm^{-1} upon cooling from 300 to 5 K due to increase in the CF strength, the energies of the Stark levels at 5 K are expected to be a few cm^{-1} smaller than estimated above. The analysis of hot bands confirms therefore the presence of the Stark levels near 291, 355, and 466 cm^{-1} , established from the luminescence spectra, and shows that one of the missing levels is located near 170 cm^{-1} . The energy difference of 94 cm^{-1} could correspond to the second Stark level. However, no hot band corresponding to such energy difference is observed for the ${}^6\text{H}_{15/2} \rightarrow {}^4\text{F}_{9/2}$ transition. Therefore, the hot band corresponding to the 94 cm^{-1} energy difference could be alternatively assigned to the transition between the first excited levels of the ${}^6\text{H}_{15/2}$ and ${}^6\text{H}_{11/2}$ manifolds.

The above results show that there is a CF level at 291 cm^{-1} , in very good agreement with our Raman data. In the pyrochlore structure Dy^{3+} ion occupies sites of D_{3d} symmetry and the ground manifold ${}^6\text{H}_{15/2}$ splits into eight Kramers doublets $3\Gamma_{56} + 5\Gamma_4$. According to literature data, the ground level has Γ_{56} symmetry.^{37,39} A transition between two electronic levels is Raman allowed if the direct product of their representations contains some of the irreducible representations of the Raman-active phonons. In the case of $\text{Dy}_2\text{Ti}_2\text{O}_7$ the direct product of the ground and excited levels is either $\Gamma_{56} \times \Gamma_{56} = 2A_1 + 2A_2$ or $\Gamma_{56} \times \Gamma_4 = 2E$, which corresponds for the $Fd\bar{3}m$ phase to $2A_{1g} + 2A_{2g} + 2F_{2g} + 2F_{1g}$ or $2E_g + 2F_{1g} + 2F_{2g}$ symmetry, respectively. As can be noticed, these two types of CF transitions should be observed both in the $x(zz)x$ configuration ($A_{1g} + E_g$ symmetry) and in the $x(zy)x$ configuration (F_{2g} symmetry). These selection rules are consistent with the polarization behavior of the 287 cm^{-1} band observed in our Raman spectra. The above discussion shows that the 287 cm^{-1} band can be assigned to the CF transition from the ground level to the excited level of energy 287 cm^{-1} .

Let us now discuss shortly why Saha *et al.*¹⁸ observed wave number shift of this band when ${}^{16}\text{O}$ is replaced by ${}^{18}\text{O}$. Since all first-order modes in pyrochlores are due to vibrations of oxygen atoms,²⁸ all wave numbers should shift downward by an amount that depends on how much O^{18} has entered the sample. The statement of Saha *et al.*¹⁸ that the sample gained almost 2% of weight indicates that about 75% of ${}^{16}\text{O}$ have been exchanged by ${}^{18}\text{O}$, giving the average oxygen mass of 17.5. Therefore, wave numbers should be downshifted by a factor $(16/17.5)^{0.5} = 0.956$. This means that the bands at 287, 311, and 329 cm^{-1} (at 5 K) should shift to 274.4, 297.3, and 314.5 cm^{-1} . The observed shifts of the 311 and 329 cm^{-1} phonon modes in Ref. 18 are in very good agreement with the expectations. However the band near 287 cm^{-1} shifts by only 4 cm^{-1} , instead of the expected 12.6 cm^{-1} . This small shift can be most likely explained in the following way. As mentioned above, the 287 cm^{-1} band has strong contribution of F_{2g} symmetry. It is therefore al-

lowed to couple to the F_{2g} mode at 311 cm^{-1} . For the ^{16}O rich sample this coupling is weak (see discussion in the next paragraphs) due to the large energy separation between these bands. However, in the ^{18}O rich sample the F_{2g} mode shifts downward considerably, approaching the energy of the uncoupled CF transition, thus enhancing the CF-phonon coupling which results in a slight redshift of the CF band.

The second argument used by Saha *et al.*¹⁸ to attribute a phononic origin to the band at 287 cm^{-1} is the narrowing of the band in the ^{18}O enriched sample. To support this change, they cite a paper from Cardona and Ruf that would imply a dependence of the linewidth as $1/M$, M being the mass of the vibrating atom.⁴⁰ The expression given in Cardona's paper is for elemental semiconductors.⁴⁰ Since in pyrochlores only oxygen atoms vibrate, we may assume that this expression is valid in these compounds. Even so, it would give a narrowing of only $16/17.5=0.91$ times, whereas Saha *et al.*¹⁸ observed a much larger narrowing, in a ratio of $6.7/9.1=0.74$. Furthermore, the $1/M$ dependence is valid only for the contribution of the third-order anharmonic decay to the linewidth and there is another contribution much more important that comes from the disorder in atomic masses and is called the isotope-mass-fluctuation effect.^{40,41} This last effect would lead to a linewidth increase in the exchanged sample, which has 75% of ^{18}O and 25% of ^{16}O , compared to the nonenriched compound, since natural oxygen is almost 100% isotopically pure (see for instance Serrano *et al.*⁴¹). Thus the spectrum of the enriched sample should broaden, not narrow. We argue therefore that the narrowing observed by Saha *et al.*¹⁸ is not indicative of phononic origin of bands but has another explanation. In fact, the comparison of the spectra shows that the bands of the nonenriched pyrochlore are much broader for Saha's sample than for our crystal whereas the linewidths for the enriched sample are nearly the same as for our crystal. For instance, the full widths at half maximum (FWHM) of the 287 cm^{-1} band in the nonenriched,¹⁸ ^{18}O enriched and our crystal are 9.1, 6.7, and 6.5 cm^{-1} , respectively (at 12 K for the Saha's sample,¹⁸ and at 5 K for our crystal). This result may indicate that Saha's nonenriched sample is somewhat disordered, whereas the enriched sample turns to be more ordered due to the long treatment at high temperature (7 days at $950\text{ }^\circ\text{C}$,¹⁸).

C. Origin of the 300 cm^{-1} mode

Figure 5 shows that apart of the 287 cm^{-1} band at 5 K (290 cm^{-1} at 120 K), assigned by us to a CF transition, one more band appears for $\text{Dy}_2\text{Ti}_2\text{O}_7$ at about 300 cm^{-1} (at 120 K), which was not observed for the other rare-earth titanates. As can be seen in Fig. 5, this band can be clearly observed in the $x(\text{zz})x$ configuration due to good polarization of our spectra. It was overlooked in the previous studies,^{17,18,26} due to poor polarization of the spectra resulting in overlapping of this band by the much stronger F_{2g} mode near 311 cm^{-1} . By subtracting the F_{2g} spectrum of $\text{Ho}_2\text{Ti}_2\text{O}_7$ at 120 K from that of $\text{Dy}_2\text{Ti}_2\text{O}_7$ at the same temperature, we conclude that (i) the 287 and 300 cm^{-1} bands are absent in the Ho pyrochlore, and (ii) in $\text{Dy}_2\text{Ti}_2\text{O}_7$ they appear both in $x(\text{zz})x$ and in $x(\text{zy})x$ configurations. These results indicate that the 300 cm^{-1} band

is associated with the Dy^{3+} ion, similarly as the 287 cm^{-1} band. Figure 5 shows, however, that the temperature dependence of the intensity of this band is different from that observed for the 287 cm^{-1} band. In particular, the 287 cm^{-1} band decreases upon heating whereas the 300 cm^{-1} band is not observed at 5 K, its intensity increases upon heating up to about 160 K and then decreases. The intensity of a CF transition is proportional to the population of the initial electronic state. Thus, the intensity of a transition starting from the ground level is largest at 0 K and decreases upon heating due to depopulation of this level. This behavior is observed for the 287 cm^{-1} band, which could be attributed to the transition from the ground level of the split ${}^6\text{H}_{15/2}$ manifold to the excited level of this manifold. Transitions from an excited level are not observed at 0 K and they gain intensity upon heating until, in their turn, they may also lose intensity as higher levels become populated. Figure 5 shows that this behavior is observed for the 300 cm^{-1} band and therefore it can be attributed to transition from one excited level to another excited level of higher energy. Since the ratio of populations of any two Stark levels within a manifold is $N_a/N_b = \exp(E_b - E_a/kT)$ and the intensity of a CF transition is proportional to the population of the initial electronic state, the intensity ratio $I(\text{band at } 300\text{ cm}^{-1})/I(\text{band at } 287\text{ cm}^{-1}) = \exp(-E_a/kT)$, where E_a is the energy of the CF level serving as initial state for the transition seen at 300 cm^{-1} . Integrated intensities of the bands at 287 and 300 cm^{-1} were estimated by fitting the spectra as a sum of Lorentzian profiles in the region from 250 to 400 cm^{-1} . An Arrhenius plot of the intensity ratio I_{300}/I_{287} from 50 to 160 K gives an activation energy E_a of 227 K, i.e., 158 cm^{-1} , with an error of about $\pm 10\text{ cm}^{-1}$. This energy is close to the CF level found at about 170 cm^{-1} from the absorption spectra. We can, therefore, attribute the band at 300 cm^{-1} to transition between the Stark levels at about 170 and 466 cm^{-1} .

D. Temperature dependence of phonon linewidths and wave numbers

Figures 7(a)–7(f) show the temperature dependence of wave numbers of the three most intense Raman modes for Dy and Ho titanates, respectively. The insets show the corresponding linewidths. It can be seen that the bands broaden monotonously with increasing temperature in quite a similar way in both compounds. However, the temperature evolution of the Raman shifts is unconventional in several aspects: a continuous hardening of the A_{1g} mode is observed upon heating, whereas for E_g and F_{2g} modes an initial hardening is followed, above a certain crossover temperature, by the more common behavior of mode softening with increasing temperature due to lattice expansion.

Rare earth titanates are well ordered, insulating materials. Thus, the change in damping and phonon wave numbers with temperature is expected to come mainly from spin-phonon anharmonic contribution, CF-phonon coupling and phonon-phonon anharmonic effects.^{26,27}

As discussed in our previous papers, spin-phonon coupling effects may be significant only when appreciable magnetic correlations exist.^{26,27} For $\text{Ho}_2\text{Ti}_2\text{O}_7$ the short-range

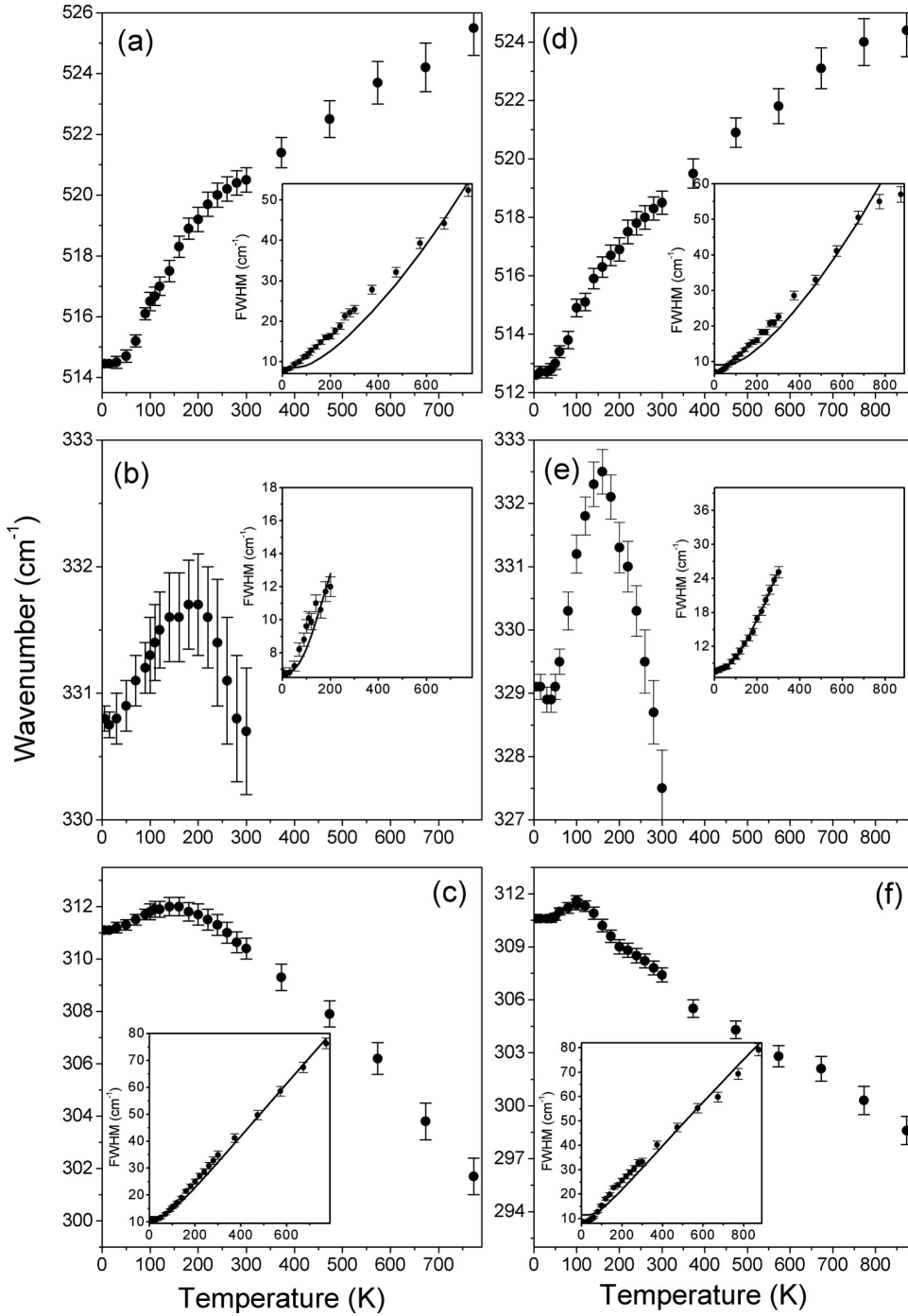


FIG. 7. Variation with temperature of the Raman peak positions of $\text{Ho}_2\text{Ti}_2\text{O}_7$ (panels a, b, and c) and $\text{Dy}_2\text{Ti}_2\text{O}_7$ (panels d, e, and f). The insets show the corresponding linewidths.

magnetic correlation becomes significant with decreasing temperature at around 30 K and for $\text{Dy}_2\text{Ti}_2\text{O}_7$ a spin freezing occurs at 16 K.^{16,42} Therefore, the spin-phonon coupling may contribute weakly to the observed damping and shifts of phonon modes only at low temperatures, typically below 30 K.

Regarding CF-phonon coupling, we may compare the results for Dy and Ho titanates with those of $\text{Tb}_2\text{Ti}_2\text{O}_7$, where strong coupling between the intense F_{2g} mode and some CF excitations were detected,²⁷ and with those observed for $\text{Gd}_2\text{Ti}_2\text{O}_7$,²⁶ for which there is no a level splitting due to the local crystal field for Gd^{3+} . In $\text{Tb}_2\text{Ti}_2\text{O}_7$, unusually large linewidths were found even at the lowest temperatures, which was attributed to CF-phonon coupling. This broaden-

ing is not observed either for $\text{Ho}_2\text{Ti}_2\text{O}_7$ nor for $\text{Dy}_2\text{Ti}_2\text{O}_7$, whose Raman bands become narrow at low temperature, as in $\text{Gd}_2\text{Ti}_2\text{O}_7$.²⁶ This suggests that the CF-phonon contribution to the damping is negligible for these phonons.

The evolution of the Raman shifts also supports this conclusion since both at RT and at 5 K the frequencies of the three intense modes are almost the same as in other pyrochlores, implying that they are not shifted by CF-phonon coupling.

This conclusion may be somewhat surprising, since, in principle, CF-phonon coupling effects would be expected in $\text{Dy}_2\text{Ti}_2\text{O}_7$, where we have assigned the band near 287 cm⁻¹ to a CF excitation (see Sec. III B). As shown above, the

coupling of this band to the F_{2g} phonon mode at 307 cm^{-1} is allowed by symmetry. If present, it should lead to a significant shift of the F_{2g} mode toward higher wave numbers, the shift decreasing with increasing temperature. Figure 7 shows that the F_{2g} mode shifts below 100 K to lower wave numbers, i.e., in the opposite way than expected in the presence of the CF-phonon coupling.

Thus we conclude that the only relevant terms to explain the temperature dependence of both linewidths and wave numbers are those due to lattice anharmonicity, either of quasiharmonic type, related to the temperature evolution of structural parameters, or true anharmonicity, arising from third- or fourth-order anharmonic decay.

The contribution of the third- and fourth-order anharmonicity to the linewidths, under the assumption that decay occurs to 2 or 3 phonons of equal energy, amounts to⁴³

$$\Gamma(T) = \Gamma_0 + C \left(1 + \frac{2}{e^x - 1} \right) + D \left(1 + \frac{3}{e^y - 1} + \frac{3}{(e^y - 1)^2} \right), \quad (1)$$

where $x = E/2k_B T$, $y = E/3k_B T$, and E is the energy of the decaying phonon. k_B and T denote the Boltzmann constant and the temperature, respectively. Γ_0 accounts for the broadening arising from factors other than the phonon decay, such as structural or compositional defects. The coefficients C and D are adjustable parameters that represent the strengths of the third- and fourth-order phonon-phonon interactions, respectively.

The fitting parameters Γ_0 , C , and D for the F_{2g} mode are (0.3, 11.6, 0.03) for $\text{Ho}_2\text{Ti}_2\text{O}_7$ and (0.3, 11.2, -0.06) for $\text{Dy}_2\text{Ti}_2\text{O}_7$. For the E_g mode the parameters are (0.6, 6.2, 0.1) for $\text{Ho}_2\text{Ti}_2\text{O}_7$ and (0.6, 7.0, 0.55) for $\text{Dy}_2\text{Ti}_2\text{O}_7$ and for the A_{1g} they are (0.1, 7.8, 0.7) and (0.1, 8.3, 0.8) for Ho and Dy pyrochlores, respectively. Large values of C parameters and small values of Γ_0 indicate that $\text{Ho}_2\text{Ti}_2\text{O}_7$ and $\text{Dy}_2\text{Ti}_2\text{O}_7$ have strong third-order anharmonicity and small concentration of structural defects. It is worth noting that the temperature dependence of the $\text{Ho}_2\text{Ti}_2\text{O}_7$ and $\text{Dy}_2\text{Ti}_2\text{O}_7$ linewidths is very similar to the temperature dependence of the corresponding modes of $\text{Er}_2\text{Ti}_2\text{O}_7$ and $\text{Gd}_2\text{Ti}_2\text{O}_7$.²⁶ This result shows that replacement of Er^{3+} or Gd^{3+} by Ho^{3+} or Dy^{3+} has very little effect on the analyzed phonons and the anharmonic interactions.

With the above discussed assumptions the wave number of a phonon i is given by

$$\omega_i(T) = \omega_{i0} + (\Delta\omega_i)_{\text{latt}} + (\Delta\omega_i)_{\text{anh}}, \quad (2)$$

where ω_{i0} is the harmonic frequency. The quasiharmonic term $(\Delta\omega_i)_{\text{latt}}$ accounts for the change of the ionic binding energies due to lattice expansion and thermal evolution of other structural parameters, and $(\Delta\omega_i)_{\text{anh}}$ is the intrinsic (or true) anharmonic contribution.

The third term, in the assumption of anharmonic decay to two or three phonons of equal energy, is given by⁴³

$$\Delta\omega_{i,\text{anh}}(T) = A \left(1 + \frac{2}{e^x - 1} \right) + B \left(1 + \frac{3}{e^y - 1} + \frac{3}{(e^y - 1)^2} \right), \quad (3)$$

where x , y have the same meaning as in Eq. (1), and A and B represent the strength of third- and fourth-order decays, respectively. Depending on the magnitude and signs of A and B this contribution may be positive or negative. In any case, both terms tend to saturate at low temperatures, typically below 100 K, so that Eq. (3) alone cannot explain the evolution of Raman shifts shown in Fig. 7, especially at low temperatures.

As regards the lattice contribution (quasiharmonic term), it is usually expressed as

$$\Delta\omega_{gh}^i(T) = \omega_{i0} \left\{ \exp \left[- \int_0^T \gamma_i \alpha(T') dT' \right] - 1 \right\}, \quad (4)$$

where

$$\gamma_i = - \frac{\partial \ln \omega_i}{\partial \ln V}$$

is the Grüneisen parameter of mode i and

$$\alpha(T) = \frac{1}{V} \frac{\partial V}{\partial T}$$

is the coefficient of thermal expansion. If γ and α are positive the exponential is < 1 and this contribution is negative; this is the common behavior in positively expanding lattices. However, if either γ or α are negative the shift is positive, as occurs for instance in systems with negative thermal expansion.⁴⁴

Positive Grüneisen parameters have been reported from Raman measurements under pressure for $\text{Dy}_2\text{Ti}_2\text{O}_7$ (Ref. 18) and very recently also for $\text{Tb}_2\text{Ti}_2\text{O}_7$ (Ref. 45) so that we may assume that they will also be positive for $\text{Ho}_2\text{Ti}_2\text{O}_7$. As regards thermal expansion coefficients, an almost constant lattice parameter is found at low T (≤ 50 K) followed by a positive lattice expansion above that temperature,¹³ so that $\alpha \geq 0$. Then, Eq. (4) alone predicts a constant frequency at low temperature followed by the usual softening with increasing temperatures, which is contrary to the observation for the A_{1g} mode at any T and for the E_g and F_{2g} (310 cm^{-1}) modes at low temperature.

The A_{1g} mode shows a monotonous hardening upon increasing temperature. Positive shifts are also observed for the overtones near 175–212 and 670–730 cm^{-1} . The same behavior is observed for many other $A_2\text{Ti}_2\text{O}_7$ pyrochlores as those with $A = \text{Gd}$, Er , Tb ,^{26,27} Y , and Yb (unpublished data) and Lu ,¹⁸ but no anomalous increase of the A_{1g} frequency could be found for KOs_2O_6 , $\text{Y}_2\text{Ru}_2\text{O}_7$, A_2MnO_7 or $\text{Cd}_2\text{Re}_2\text{O}_7$ pyrochlores.^{20,35,46,47}

The hardening of the A_{1g} mode might be explained by means of Eqs. (3) and (4) as a result of unusually strong and positive intrinsic anharmonicity, as proposed in the recent studies of $\text{Dy}_2\text{Ti}_2\text{O}_7$ and $\text{Lu}_2\text{Ti}_2\text{O}_7$,¹⁸ but these equations cannot reproduce the fast decrease of the Raman shift below 150 K, since anharmonic interactions tend to slow down as

temperature is lowered. A combination of Eqs. (3) and (4) might also explain the behavior of the F_{2g} and E_g modes at high temperatures, but not the downturn observed at low temperature.

It seems that the Raman shifts shown in Fig. 7 cannot be explained by Eqs. (3) and (4), neither separately nor combined. Particularly puzzling is the changing trend observed at a crossover temperature of about 100–150 K for all modes. It is worth noting that very similar behavior was observed for $Gd_2Ti_2O_7$, $Er_2Ti_2O_7$, and $Tb_2Ti_2O_7$,^{26,27} and also reported for $Dy_2Ti_2O_7$ and $Lu_2Ti_2O_7$ by Saha *et al.*¹⁸

The question that arises is what the origin of this anomaly is. Some negative shift may result from the spin-phonon anharmonic interactions at low temperatures^{22,26,27,48} However, as discussed above, the spin-phonon coupling is expected to be negligible above ~ 30 K in these materials,²⁶ whereas the anomalous Raman results extend up to much higher temperatures (100–150 K). Moreover, the effect is observed in pyrochlores with very different magnetic properties, and also in nonmagnetic compounds, such as $Lu_2Ti_2O_7$.¹⁸ Then, we conclude that it has a nonmagnetic origin and search an explanation based only on structural properties.

In their recent paper, Saha *et al.*¹⁸ attributed the observed anomaly in $Dy_2Ti_2O_7$ to a subtle structural transformation near 110 K, which would lead to a discontinuity in the lattice parameter. If this explanation is correct, the temperature dependence of phonon modes in other $A_2Ti_2O_7$ pyrochlores ($A=Ho, Gd, Er, Tb$) would imply that these materials undergo a similar structural change as $Dy_2Ti_2O_7$ at about 100–130 K. However, to the authors' knowledge there are no reports on structural transformations for these pyrochlores. Furthermore, structural studies of $Tb_2Ti_2O_7$ could not reveal any discontinuity in the lattice parameter and some anomalous, continuous behavior was observed only below 18 K.^{11,49}

We propose an explanation based on a closer examination of the pyrochlore geometry and its relation with the Raman activity. The idea stems from noting that Eq. (4) depends on the average lattice expansion coefficient, α , so that it does not account for the thermal evolution of the internal coordinates involved in each particular vibration. With the usual formulation, the quasiharmonic contribution to the variation of ω_i with T is⁴⁴

$$\left(\frac{d\omega_i}{dT}\right)_{\text{quasih}} = \left.\frac{\partial\omega_i}{\partial V}\right|_T \left.\frac{\partial V}{\partial T}\right|_P = -\omega_i\gamma_i\alpha.$$

To take into account the variation of internal coordinates we reformulate this expression as

$$\left(\frac{d\omega_i}{dT}\right)_{\text{quasih}} = \left.\frac{\partial\omega_i}{\partial Q_i}\right|_T \left.\frac{\partial Q_i}{\partial T}\right|_P = -\omega_i\gamma_{Q_i}\alpha_{Q_i},$$

where Q_i is the normal coordinate of mode i and we have introduced effective Grüneisen and thermal expansion parameters for each mode

$$\gamma_{Q_i} = -\frac{\partial \ln \omega_i}{\partial \ln Q_i} \quad \text{and} \quad \alpha_{Q_i}(T) = \frac{1}{Q_i} \frac{\partial Q_i}{\partial T}.$$

Then, depending on the structural properties of the compound and the thermal evolution of the normal coordinates involved in each mode, the relevant parameter α_{Q_i} may have a different sign from α . We propose that this is at the origin of the anomaly in $\omega_i(T)$.

E. Discussion

The evolution of Raman shifts with temperature shown in Fig. 7 suggests that there exists a competition between two different processes or interactions, one of them producing, at high temperature, the conventional softening due to lattice expansion and the other one, extending at low temperatures up to a crossover temperature that depends on the specific mode, that produces an anomalous softening of some modes on cooling.

The situation is reminiscent of systems presenting negative thermal expansion (NTE) at low temperature, in which NTE appears as a result of the competition between stretching (valence) forces, favoring lattice expansion, and large amplitude bending or transverse vibrations that may result in lattice contraction upon temperature increase.⁵⁰

Candidates to present NTE are open framework lattices containing covalently bonded rigid units (typically MO_4 or MO_6 polyhedra) that share corners and allow for low-frequency tilting modes of such units, implying the bending of the M-O-M angles. This is the case of ZrW_2O_8 or ReO_3 .^{51,52} NTE also appears in more stiff lattices presenting two-coordinated atoms as in A-B-A chains, allowing low-frequency vibrations of the B atoms transverse to the bond direction. Examples of this behavior are delafossites⁵³ or Cu_2O and Ag_2O cristobalites.⁵⁴ These high amplitude vibrations manifest in the form of large and anisotropic thermal parameters for the low-coordinated atoms.

As far as we know, no negative thermal expansion has been reported in Ti pyrochlores. However, the pyrochlore lattice presents some structural peculiarities that relate them to systems undergoing NTE.

It is traditional to describe the pyrochlore structure as consisting of a framework of corner-sharing $BO(1)_6$ octahedra with A and O(2) atoms occupying the pseudohexagonal cages thus resulting in a $2O(2)+6O(1)$ coordination for the A cations.⁵⁵ As regards the oxygen atoms, both are four coordinated, in a perfect tetrahedron of A cations around O(2) oxygens, and in a pseudotetrahedral environment of $2A+2B$ cations for O(1) atoms. We note, however, that the A-O(1) bond distance, ~ 2.5 Å, is much longer than the A-O(2) bond (~ 2.2 Å), so that, in practice, the coordination of the A cations can be considered as linear, in the form of O(2)-A-O(2) chains along the trigonal axis. The A-O(1) bond is also much longer than the B-O(1) one (~ 2 Å), so that the O(1) atoms can be thought as being coordinated to only two Ti, forming a Ti-O-Ti angle of about 135° . Therefore, both A and O(1) atoms are candidates to perform large amplitude transverse vibrations with low frequency, similarly as in NTE systems and, in fact, they both show stronger thermal

displacements parameters than B and O(2) atoms in x-ray or EXAFS experiments.¹¹

In the limit of negligible A-O(1) interaction, the pyrochlore lattice can be described as the interpenetration of two separate networks, consisting of A-O(2) and B-O(1) sublattices, respectively.⁵⁶ Quite interestingly, the network of A and O(2) atoms is of a cristobalite type analogous to that of Cu₂O, a well-known example of NTE.⁵⁴ In Cu₂O, NTE is ascribed to the vibration of Cu atoms transverse to the O-Cu-O bonds. The analogous motion in the pyrochlore would be the vibration of A cations perpendicularly to the A-O(2) bonds. Since the A cations are not Raman active in the pyrochlores, it is unlikely that the anomalous Raman shifts can be attributed to such effect. Moreover, A and O(2) atoms occupy special positions, so that their distance is fixed by the lattice parameter. Any anomalous behavior of A atom vibrations should manifest through the thermal evolution of the lattice parameter.

For the discussion of Raman modes, it is more interesting to investigate the properties of the B-O(1) network since the major contribution to the Raman spectrum comes from O(1) vibration. In particular, only O(1) oxygens vibrate in A_{1g} and E_g modes, whose displacements are determined by symmetry.

O(1) atoms around Ti form a distorted octahedron, the degree of distortion being a function of the O(1) parameter x . For the ideal pyrochlore structure $x=0.3125$ and then the TiO₆ form a perfect octahedron,⁵⁵ whereas for the x values found in Ti pyrochlores ($x\sim 0.33$) the octahedron is compressed. The occurrence of a free parameter in the pyrochlore structure and the resulting octahedron distortion yield a dependence of bond distances and angles on x that may be determinant for Raman properties. Depending on its sign, the variation of x with temperature may be opposite to that arising from lattice expansion.

Taking the origin at a Ti atom, the coordinates of its six oxygen nearest neighbors are O1($-x+1/4, 1/8, 1/8$), O2($1/8, -x+1/4, 1/8$), O3($1/8, 1/8, -x+1/4$), O4($x-1/4, -1/8, -1/8$), O5($-1/8, -1/8, x-1/4$), O6($-1/8, x-1/4, -1/8$), giving a Ti-O distance $d_{\text{Ti-O}}=\sqrt{(x-1/4)^2+1/32}$. Octahedron distortion results in two different O-O distances, a “short” one $d_{\text{O-O}}=\sqrt{2x^2-3x/2+11/32}$ and a “long” one $d'_{\text{O-O}}=\sqrt{2x^2-x/2+1/32}$. Similarly, two different O-Ti-O angles form, $\alpha < 90^\circ$ given by $\cos \alpha = (x/4 - 5/64)/d_{\text{Ti-O}}^2$, and $\alpha' = 180 - \alpha > 90^\circ$. Finally, each O(1) atom connects two different octahedra, forming a Ti-O-Ti angle given by $\cos \beta = [(x-1/4)^2 - 1/32]/d_{\text{Ti-O}}^2$. For typical values of x in Ti pyrochlores $d_{\text{Ti-O}} \sim 1.95$ Å, $d_{\text{O-O}} \sim 2.6$ Å, $d'_{\text{O-O}} \sim 2.8$ Å and $\beta \sim 135^\circ$.

The most interesting question for Raman discussion is how these coordinates change as x changes with temperature. Although no data on the change of the x parameter are available for Dy₂Ti₂O₇ and Ho₂Ti₂O₇, temperature dependent structural studies of Tb₂Ti₂O₇ revealed that this parameter decreases upon heating,¹¹ i.e., the octahedron becomes more regular as T is increased. Then, for constant lattice parameter, $d_{\text{Ti-O}}$ would decrease on heating. This trend, however, is compensated in Tb₂Ti₂O₇ by positive lattice expansion,¹¹ thus resulting in an almost constant Ti-O bond distance between 45 and 300 K. As regards the other parameters, we

note that, upon decreasing x , the O-Ti-O angle α increases but α' decreases symmetrically so that their contribution to the Raman shifts through bond-bending force constants would probably compensate. O-O distances, on the contrary, behave more interestingly, since their change is not at all symmetric: the long O-O bond will decrease upon decreasing x much more than the short O-O distance will increase, thus producing a net increase of O-O interaction. The thermal evolution of $d_{\text{Ti-O}}$ and other internal coordinates of the B-O(1) network in other A₂Ti₂O₇ pyrochlores will depend on how x and a change with temperature. Since all these compounds share similar structural characteristics we may assume that they will behave in a similar way as in Tb₂Ti₂O₇. For Dy₂Ti₂O₇ and Ho₂Ti₂O₇, for instance, the lattice parameters have been found to be almost constant below ~ 50 K,¹³ so that a decrease in x might result in a slight decrease of $d_{\text{Ti-O}}$ upon heating in this T range.

According to the calculations of Gupta *et al.*,³⁰ none of the Raman-active modes in A₂Ti₂O₇ pyrochlores involves the predominant contribution of Ti-O bond stretching, though the force constant for this vibration is strong. The main contribution to the Raman shifts of pyrochlores comes from O-Ti-O bond-bending, Ti-O bond stretching and, in particular for Ti pyrochlores, also from O-O second-neighbor interaction.

The case of the A_{1g} mode is particularly interesting since, by symmetry, this mode consists just of the modulation of the oxygen x parameter, i.e., of the octahedron distortion. In this motion, all B-O(1) coordinates are affected, so that its energy involves O-Ti-O bending and Ti-O and O-O stretching force constants. Alternatively, it can be regarded as the symmetric breathing motion of the O(1) octahedron toward the vacant 8a site at (1/8,1/8,1/8), separated from O(1) by $d_{8a-48f}=x-1/8$, so that the A_{1g} mode involves just the stretching of the O(1)-vacancy “bond” whereas the E_g mode consists of the asymmetric stretching of the O(1) octahedron centered at the vacancy.⁴⁶ With this description, the hardening of the A_{1g} mode frequency with increasing temperature would be naturally ascribed to the decrease in x . In fact, our own lattice dynamics calculations (not discussed in this paper) indicate that a decrease in the x parameter should lead to an appreciable increase of the A_{1g} and A_{2u} modes energies (5 cm⁻¹ from 45 to 400 K) and also, but much weaker, for the E_g and F_{2g} modes. This result indicates that the hardening of the A_{1g} mode and the overtones of the A_{2u} mode near 670–730 cm⁻¹ upon heating can be most likely attributed to the change in the x parameter. For the A_{1g} mode, the positive shift due to the temperature variation of x dominates at all temperatures, at least in the range studied, whereas for the E_g and 310- cm⁻¹ F_{2g} modes the initial hardening of the force constants with increasing temperature is surpassed above 100–150 K by the net softening induced by lattice expansion and intrinsic anharmonic contribution.

In the light of these arguments, we suggest that the discontinuity in the lattice parameter of Dy₂Ti₂O₇ reported in Ref. 18 may be due to the freezing of some O(1) vibration possibly producing also a small discontinuity in the oxygen parameter x . This is a very interesting possibility, closely in the line of phenomena yielding NTE, that deserves further structural studies. At a difference with systems showing

NTE, where the rigidity of polyhedra imposes large amplitude variations of interpolyhedra angles, the presence of the free oxygen parameter x in pyrochlores provides the BO_6 octahedra some degree of plasticity that allows the octahedron distortion to vary with temperature with no anomalous lattice contraction.

In summary, we ascribe the anomaly in the Raman shifts at low temperature to a combination of factors: (i) Raman-active modes have a strong bond-bending character in $\text{A}_2\text{B}_2\text{O}_7$ pyrochlores. (ii) O-Ti-O bond-bending and O-O second-neighbor force constants are much stronger in titanates than in other pyrochlores and have a magnitude comparable to that of Ti-O bond stretching. (iii) There exists a free coordinate (the oxygen parameter x) that allows the distortion of TiO_6 octahedra without affecting the long-range cubic structure. Thus, the Raman frequencies reflect the anomalous variation of internal coordinates involving the parameter x , despite the macroscopic structure presents a “normal” positive expansion. It is clear that more detailed crystallographic studies at low temperature are clearly required, preferably using local probes such as EXAFS.

IV. CONCLUSIONS

Temperature-dependent Raman scattering studies of $\text{Ho}_2\text{Ti}_2\text{O}_7$ and $\text{Dy}_2\text{Ti}_2\text{O}_7$ single crystals were performed in the 5–873 K range as well as at room temperature for $\text{Gd}_2\text{Ti}_2\text{O}_7$. Some luminescence and absorption spectra were presented to obtain information on Stark levels of the ground manifold. Our results show that the Raman selection rules are well fulfilled for $\text{Dy}_2\text{Ti}_2\text{O}_7$ and $\text{Gd}_2\text{Ti}_2\text{O}_7$ and slightly worse for $\text{Ho}_2\text{Ti}_2\text{O}_7$. The study of well oriented single crystals under polarized light and in a very broad temperature

range allowed for very precise assignment of modes and correction of numerous errors present in the literature. In particular, we have shown that the previous assignment of the band at about 287 cm^{-1} for $\text{Dy}_2\text{Ti}_2\text{O}_7$ to a new phonon mode appearing due to local symmetry lowering below 110 K is incorrect. This mode should be assigned to the CF transition from the ground level of the split ${}^6\text{H}_{15/2}$ manifold to the excited level of this manifold. We have also shown that the coupling between this transition and the F_{2g} mode near 307 cm^{-1} is weak but it is enhanced for the ${}^{18}\text{O}$ rich sample resulting in a slight redshift of the CF band. Our spectra revealed also the presence of another, previously not observed for $\text{Dy}_2\text{Ti}_2\text{O}_7$ band near 300 cm^{-1} , which can be attributed to the CF transition from one excited level to another excited level of the ${}^6\text{H}_{15/2}$ manifold.

The obtained results revealed that phonon wave numbers and linewidths in $\text{Ho}_2\text{Ti}_2\text{O}_7$ and $\text{Dy}_2\text{Ti}_2\text{O}_7$ exhibit very similar temperature dependence as those of $\text{Gd}_2\text{Ti}_2\text{O}_7$ and $\text{Er}_2\text{Ti}_2\text{O}_7$, in spite of significant differences in the magnetic properties of these materials. The softening of the A_{1g} mode with decreasing temperature and the additional anomalous decrease of the phonon wave numbers for all modes at low temperatures is attributed to the increase of octahedral distortion upon cooling.

ACKNOWLEDGMENTS

K.M. was supported by the Visiting Researcher’s Program of Institute for Solid State Physics, University of Tokyo. Crystal growth was performed using facilities of the Materials Design and Characterization Laboratory, Institute for Solid State Physics, University of Tokyo. M.L.S. acknowledges financial support from Spanish project under Grant No. MAT2007-64486-C07-02.

¹J. E. Greedan, *J. Alloys Compd.* **408-412**, 444 (2006).

²S. Singh, S. Saha, S. K. Dhar, R. Suryanarayanan, A. K. Sood, and A. Revcolevschi, *Phys. Rev. B* **77**, 054408 (2008).

³T. Fennell, O. A. Petrenko, B. Frak, S. T. Bramwell, M. Enjalran, T. Yavors’kii, M. J. P. Gingras, R. G. Melko, and G. Balakrishnan, *Phys. Rev. B* **70**, 134408 (2004).

⁴A. P. Ramirez, A. Hayashi, R. J. Cava, R. Siddharthan, and B. S. Shastry, *Nature* **399**, 333 (1999).

⁵S. T. Bramwell, M. J. Harris, B. C. den Hertog, M. J. P. Gingras, J. S. Gardner, D. F. McMorrow, A. R. Wildes, A. Cornelius, J. D. M. Champion, R. G. Melko, and T. Fennell, *Phys. Rev. Lett.* **87**, 047205 (2001).

⁶S. T. Bramwell, M. N. Field, and I. P. Parkin, *J. Phys.: Condens. Matter* **12**, 483 (2000).

⁷J. D. M. Champion, M. J. Harris, P. C. W. Holdsworth, A. S. Wills, G. Balakrishnan, S. T. Bramwell, E. Čížmár, T. Fennell, J. S. Gardner, J. Lago, D. F. McMorrow, M. Orendáč, A. Orendáčová, D. McK. Paul, R. I. Smith, M. T. F. Telling, and A. Wildes, *Phys. Rev. B* **68**, 020401(R) (2003).

⁸J. D. M. Champion, A. S. Wills, T. Fennell, S. T. Bramwell, J. S. Gardner, and M. A. Green, *Phys. Rev. B* **64**, 140407(R) (2001).

⁹N. P. Raju, M. Dion, M. J. P. Gingras, T. E. Mason, and J. E.

Greedan, *Phys. Rev. B* **59**, 14489 (1999).

¹⁰J. S. Gardner, B. D. Gaulin, A. J. Berlinsky, P. Waldron, S. R. Dunsiger, N. P. Raju, and J. E. Greedan, *Phys. Rev. B* **64**, 224416 (2001).

¹¹S. W. Han, J. S. Gardner, and C. H. Booth, *Phys. Rev. B* **69**, 024416 (2004).

¹²K. C. Rule, J. P. C. Ruff, B. D. Gaulin, S. R. Dunsiger, J. S. Gardner, J. P. Clancy, M. J. Lewis, H. A. Dabkowska, I. Mirebeau, P. Manuel, Y. Qiu, and J. R. D. Copley, *Phys. Rev. Lett.* **96**, 177201 (2006).

¹³L. G. Mamsurova, K. S. Pigalskii, N. G. Trusevich, and L. G. Shcherbakova, *Sov. Phys. Solid State* **27**, 978 (1985).

¹⁴G. Ehlers, J. S. Gardner, C. H. Booth, M. Daniel, K. C. Kam, A. K. Cheetham, D. Antonio, H. E. Brooks, A. L. Cornelius, S. T. Bramwell, J. Lago, W. Häußler, and N. Rosov, *Phys. Rev. B* **73**, 174429 (2006).

¹⁵M. J. Harris, S. T. Bramwell, D. F. McMorrow, T. Zeiske, and K. W. Godfrey, *Phys. Rev. Lett.* **79**, 2554 (1997).

¹⁶M. Kanada, Y. Yasui, Y. Kondo, S. Iikubo, M. Ito, H. Harashina, M. Sato, H. Okumura, K. Kakurai, and K. Kadowaki, *J. Phys. Soc. Jpn.* **71**, 313 (2002).

¹⁷T. T. A. Lummen, I. P. Handayani, M. C. Donker, D. Fausti, G.

- Dhalenne, P. Berthet, A. Revcolevschi, and P. H. M. van Loosdrecht, *Phys. Rev. B* **77**, 214310 (2008).
- ¹⁸S. Saha, S. Singh, B. Dkhil, S. Dhar, R. Suryanarayanan, G. Dhalenne, A. Revcolevschi, and A. K. Sood, *Phys. Rev. B* **78**, 214102 (2008).
- ¹⁹N. J. Hess, B. D. Begg, S. D. Conradson, D. E. McCready, P. L. Gassman, and W. J. Weber, *J. Phys. Chem. B* **106**, 4663 (2002).
- ²⁰J. S. Bae, I.-S. Yang, J. S. Lee, T. W. Noh, T. Takeda, and R. Kano, *Vib. Spectrosc.* **42**, 284 (2006).
- ²¹J. S. Lee, T. W. Noh, J. S. Bae, I.-S. Yang, T. Takeda, and R. Kanno, *Phys. Rev. B* **69**, 214428 (2004).
- ²²J. Laverdiere, S. Jandl, A. A. Mukhin, V. Yu. Ivanov, V. G. Ivanov, and M. N. Iliev, *Phys. Rev. B* **73**, 214301 (2006).
- ²³P. C. Becker, G. M. Williams, N. M. Edelstein, J. A. Koningstein, L. A. Boatner, and M. M. Abraham, *Phys. Rev. B* **45**, 5027 (1992).
- ²⁴M. N. Iliev, A. P. Litvinchuk, H. G. Lee, C. W. Chu, A. Barry, and J. M. D. Coey, *Phys. Rev. B* **60**, 33 (1999).
- ²⁵J. M. Wesselinowa and A. T. Apostolov, *J. Phys.: Condens. Matter* **8**, 473 (1996).
- ²⁶M. Mączka, J. Hanuza, K. Hermanowicz, A. F. Fuentes, K. Matsuhira, and Z. Hiroi, *J. Raman Spectrosc.* **39**, 537 (2008).
- ²⁷M. Mączka, M. L. Sanjuán, A. F. Fuentes, K. Hermanowicz, and J. Hanuza, *Phys. Rev. B* **78**, 134420 (2008).
- ²⁸M. Glerup, O. F. Nielsen, and F. W. Poulsen, *J. Solid State Chem.* **160**, 25 (2001).
- ²⁹R. Loudon, *Adv. Phys.* **13**, 423 (1964).
- ³⁰H. C. Gupta, S. Brown, N. Rani, and V. B. Gohel, *J. Raman Spectrosc.* **32**, 41 (2001).
- ³¹H. C. Gupta and S. Brown, *J. Phys. Chem. Solids* **64**, 2205 (2003).
- ³²S. Saha, D. V. S. Muthu, C. Pascanut, N. Dragoe, R. Suryanarayanan, G. Dhalenne, A. Revcolevschi, S. Karmakar, S. M. Sharma, and A. K. Sood, *Phys. Rev. B* **74**, 064109 (2006).
- ³³S. P. S. Porto, P. A. Fleury, and T. C. Damen, *Phys. Rev.* **154**, 522 (1967).
- ³⁴H. C. Gupta and N. Rani, *J. Phys. Chem. Solids* **68**, 1293 (2007).
- ³⁵E. Granado, P. G. Pagliuso, J. A. Sanjurjo, C. Rettori, M. A. Subramanian, S. W. Cheong, and S. B. Oseroff, *Phys. Rev. B* **60**, 6513 (1999).
- ³⁶P. Alonso-Gutiérrez and M. L. Sanjuán, *Phys. Rev. B* **76**, 165203 (2007).
- ³⁷Y. M. Jana, A. Sengupta, and D. Ghosh, *J. Magn. Magn. Mater.* **248**, 7 (2002).
- ³⁸S. Rosenkranz, A. P. Ramirez, A. Hayashi, R. J. Cava, R. Sidharthan, and B. S. Shastry, *J. Appl. Phys.* **87**, 5914 (2000).
- ³⁹B. Z. Malkin, A. R. Zakirov, M. N. Popova, S. A. Klimin, E. P. Chukalina, E. Antic-Fidancev, Ph. Goldner, P. Aschehoug, and G. Dhalenne, *Phys. Rev. B* **70**, 075112 (2004).
- ⁴⁰M. Cardona and T. Ruf, *Solid State Commun.* **117**, 201 (2001).
- ⁴¹J. Serrano, F. J. Manjón, A. H. Romero, F. Widulle, R. Lauck, and M. Cardona, *Phys. Rev. Lett.* **90**, 055510 (2003).
- ⁴²J. Synder, B. G. Ueland, J. S. Slusky, H. Karunadasa, R. J. Cava, and P. Schiffer, *Phys. Rev. B* **69**, 064414 (2004).
- ⁴³M. Balkanski, R. F. Wallis, and E. Haro, *Phys. Rev. B* **28**, 1928 (1983).
- ⁴⁴T. R. Ravindran, A. K. Arora, and T. A. Mary, *Phys. Rev. B* **67**, 064301 (2003).
- ⁴⁵S. Saha, D. V. S. Muthu, S. Singh, B. Dkhil, R. Suryanarayanan, G. Dhalenne, H. K. Poswal, S. Karmakar, S. M. Sharma, A. Revcolevschi, and A. K. Sood, *Phys. Rev. B* **79**, 134112 (2009).
- ⁴⁶T. Hasegawa, Y. Takasu, N. Ogita, M. Udagawa, J. I. Yamaura, Y. Nagao, and Z. Hiroi, *Phys. Rev. B* **77**, 064303 (2008).
- ⁴⁷C. S. Knee, J. Holmlund, J. Andreasson, M. Käll, S. G. Eriksson, and L. Börjesson, *Phys. Rev. B* **71**, 214518 (2005).
- ⁴⁸E. Granado, N. O. Moreno, A. Garcia, J. A. Sanjurjo, C. Rettori, I. Torriani, S. B. Oseroff, J. J. Neumeier, K. J. McClellan, S. W. Cheong, and Y. Tokura, *Phys. Rev. B* **58**, 11435 (1998).
- ⁴⁹J. P. C. Ruff, B. D. Gaulin, J. P. Castellan, K. C. Rule, J. P. Clancy, J. Rodriguez, and H. A. Dabkowska, *Phys. Rev. Lett.* **99**, 237202 (2007).
- ⁵⁰G. D. Barrera, J. A. O. Bruno, T. H. K. Barron, and N. L. Allan, *J. Phys.: Condens. Matter* **17**, R217 (2005).
- ⁵¹T. A. Mary, J. S. O. Evans, T. Vogt, and A. W. Sleight, *Science* **272**, 90 (1996).
- ⁵²T. Chatterji, P. F. Henry, R. Mittal, and S. L. Chaplot, *Phys. Rev. B* **78**, 134105 (2008).
- ⁵³S. I. Ahmed, G. Dalba, P. Fornasini, M. Vaccari, F. Rocca, A. Sanson, J. Li, and A. W. Sleight, *Phys. Rev. B* **79**, 104302 (2009).
- ⁵⁴A. Sanson, F. Rocca, G. Dalba, P. Fornasini, R. Grisenti, M. Dapiaggi, and G. Artioli, *Phys. Rev. B* **73**, 214305 (2006).
- ⁵⁵M. A. Subramanian, G. Aravamudan, and G. V. Subba Rao, *Prog. Solid State Chem.* **15**, 55 (1983).
- ⁵⁶J. Pannetier and J. Lucas, *Mater. Res. Bull.* **5**, 797 (1970).